Supervised Multimodal Fusion and Its Application in Searching Joint Neuromarkers of Working Memory Deficits in Schizophrenia

Shile Qi, Vince D. Calhoun, *Fellow IEEE* , Theo G. M. van Erp, Eswar Damaraju, Juan Bustillo, Yuhui Du, Jessica A. Turner, Daniel H. Mathalon, Judith M. Ford, James Voyvodic, Bryon A. Mueller, Aysenil Belger, Sarah Mc Ewen, Steven G. Potkin, Adrian Preda, FBIRN, Tianzi Jiang, Jing Sui*, *Senior* M*ember IEEE*

Abstract—**Multimodal fusion is an effective approach to better understand brain disease. To date, most current fusion approaches are unsupervised; there is need for a multivariate method that can adopt prior information to guide multimodal fusion. Here we proposed a novel supervised fusion model, called "MCCAR+jICA", which enables both identification of multimodal co-alterations and linking the covarying brain regions with a specific reference signal, *e.g.*, cognitive scores. The proposed method has been validated on both simulated and real human brain data. Features from 3 modalities (fMRI, sMRI, dMRI) obtained from 147 schizophrenia patients and 147 age-matched healthy controls were included as fusion input, who participated in the Function Biomedical Informatics Research Network (FBIRN) Phase III study. Our aim was to investigate the group co-alterations seen in three types of MRI data that are also correlated with working memory performance. One joint IC was found both significantly group-discriminating (p=7.4E-06, 0.001, 7.0E-09) and highly correlated with working memory scores(r=0.296, 0.241, 0.301) and PANSS negative scores (r=-0.229, -0.276, -0.240) for fMRI, dMRI and sMRI, respectively. Given the simulation and FBIRN results, MCCAR+jICA is shown to be an effective multivariate approach to extract accurate and stable multimodal components associated with a particular measure of interest, and promises a wide application in identifying potential neuromarkers for mental disorders.**

I. Introduction

In neuropsychological studies, evidence has been accumulated that schizophrenia (SZ) is associated with significant impairment in cognitive functioning, in which working memory (WM) is the cognitive domain showing the most pronounced deficits, and has been most severely affected in schizophrenia[1]. While most existing studies about WM deficits are based on unimodal analysis, multi-modal fusion has been a natural option to provide more clues by exploiting the relationship between rich multimodal brain imaging data with cognitive and behavior information for individual subjects, rather than performing analysis within each modality alone.

Existing multivariate multimodal fusion methods have different advantages and limitations. Specifically, multi-set CCA (MCCA) and sparse CCA maximize the inter-modality covariation across multiple types of features, but their associated source maps may not be sufficiently unique. Joint ICA (jICA), and linked ICA perform well in spatial decomposition, but all modalities share a common profile. Combining the advantages of MCCA and jICA, we already successfully developed unsupervised multimodal fusion algorithm "MCCA+jICA" [2, 3], which captures both interactions among *n* modalities and the source independence of interest and applied it to multiple cases. Other data fusion approaches like IVA [4] generalizes ICA to multiple data sets using mutual information rate that achieves a similar performance to MCCA+jICA. Parallel ICA (pICA) [5, 6] uses a similar idea, maximizing not only the inter-modality correlation but also the independence of sources under ICA framework, to specially deal with genetic data. However, all the above mentioned fusion approaches are unsupervised machine learning methods as summarized in[7] [8]. By contrast, supervised fusion of brain imaging data is more goal-directed, since it is trying to further take advantage of a prior knowledge to guide the analysis and pinpoint a particular component of interest embedded in a large complex dataset. For example, Chen proposed pICA-R (pICA with references) which used candidate genes as spatial priori to investigate the relationships between hidden factors of a particular attribute.

Besides capturing shared and unique brain regions of interest (ROIs) as well as their interactions among *n* modalities, investigators may also be interested in discovering multimodal associations with a specific reference signal, e.g., the cognitive scores or psychotic symptoms. While currently utilizing neuroimaging data to identify cognitive biomarkers has been a hot topic, linking a specific cognitive domain (*e.g.* WM) with neuroimaging data and simultaneously mining multimodal co-alterations with mental disorders remains unexplored. Therefore, if we can use WM performance as a constraint to guide the multimodal fusion, we may even be able to extract joint components specifically associated with WM domain that can help further elucidate the mechanism of WM deficits in mental disorders as well as its impairment in disease. All the above motivate our supervised multimodal fusion model, "MCCAR+jICA" (multi-set CCA with reference + joint ICA, as shown in Figure 1), which simultaneously maximize inter-modality

*Resrach supported by NIH and Chinese Academy of Sciences (CAS)

Shile Qi, Jing Sui and Tianzi Jiang are with the Brainnetome center & National Laboratory of Pattern Recognition, Institute of Automation, Chinese Academy of Sciences (corresponding author: kittysj@gmail.com).

Eswar Damaraju, Jing Sui, Yuhui Du, Jessica A. Turner, and Vince D Calhoun are with the Mind Research Network/LBERI. Dr. Calhoun is also with Dept. of ECE, University of New Mexico, Albuquerque, NM, 87106.

Theo G. M. van Erp, Steven G. Potkin , Adrian Preda and FBIRN are with Department of Psychiatry and Human Behavior, University of California Irvine, Irvine, CA, 92617.

Juan Bustillo and Jessica A. Turner are with Department of Psychiatry, University of New Mexico, Albuquerque, NM, 87131.

Daniel H. Mathalon and Judith M. Ford are with San Francisco VA Medical Center. They and FBIRN are also with Department of Psychiatry, University of California, San Francisco, San Francisco, CA, 94143.

James Voyvodic is with Department of Radiology, Brain Imaging and Analysis Center, Duke University, Durham, NC, 27710.

Bryon A. Mueller is with Department of Psychiatry, University of Minnesota, Minneapolis, MN, 55454.

Aysenil Belger is with Department of Psychiatry, University of North Carolina School of Medicine, Chapel Hill, NC, 27599.

Sarah McEwen is with Department of Psychiatry and Biobehavioral Sciences, University of California, Los Angeles, Los Angeles, CA, 90095.

978-1-4577-0220-4/16/$31.00 ©2016 IEEE

associations and optimize specific correlations under the guidance of a reference. As a result, MCCAR+jICA enables detection of a joint multimodal component(s) that has robust correlations with both reference signal and among themselves (inter-modality correlations), which may not be detected by a blind (unsupervised) N-way multimodal fusion approach.

The remaining of this paper is organized as follows: section II presents the development of MCCAR+jICA algorithm. In section III, the simulated data is used to evaluate the proposed method with its alternatives. In section 4 and 5, the application results using FBIRN data are introduced and discussed, as well as the future work. To the best of our knowledge, this is the first attempt to propose a supervised fusion model to combine three modalities of brain imaging data with a cognitive domain together, focusing on mining joint neuromarkers particularly correlated with working memory deficits in schizophrenia.

II. Methods

A. MCCAR

Assume that there are n multimodal datasets $\boldsymbol{X}_k$, $k = 1,2,\dots,n$, each is a linear mixture of components $\boldsymbol{C}_k$ with a nonsingular mixing matrix $\boldsymbol{A}_k$, k denotes modality.

$$\boldsymbol{X}_k = \boldsymbol{A}_k \boldsymbol{C}_k \quad k = 1,2,\dots,n \tag{1}$$

where $\boldsymbol{X}_k$ is a subjects-by-voxels feature matrix, $\boldsymbol{A}_k$ is in dimension of subjects by number of components M. MCCA with reference (MCCAR) imposes an additional constraint upon the MCCA framework to maximize not only the covariations among mixing matrices of each modality, but also the top column-wise correlations between $\boldsymbol{A}_k$ and the reference signal, as shown in Figure1(c).

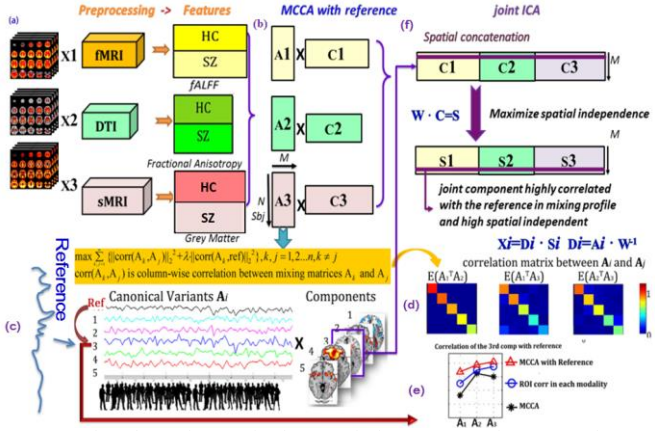

Figure 1 Flowchart of supervised 3-way fusion strategy of MCCAR+jICA.

The basic strategy of MCCAR is as follows: consider that there are N subjects, dimension reduction is first performed on $\boldsymbol{X}_k$,thus the signal subspace given by $\boldsymbol{Y}_k = \boldsymbol{X}_k \boldsymbol{E}_k$ are determined. MCCAR is thus performed on $\boldsymbol{Y}_k$, generating the canonical variants $\boldsymbol{A}_k$ by maximizing the sum of squared correlations (SSQCOR) among canonical variants (CVs) as well as the SSQCOR between each CVs and the reference signal. We can summarize the optimization procedure of MCCAR as below. Consider the CVs $\boldsymbol{A}_k$ given by $\boldsymbol{A}_k = \boldsymbol{Y}_k \boldsymbol{w}_k$ were jointly decomposed into M components, then the canonical coefficient vectors $\boldsymbol{w}_k$ are updated by two stages:

$$\text{Stage 1: } \left\{\boldsymbol{w}_1^{(1)}, \boldsymbol{w}_2^{(1)}, \cdots, \boldsymbol{w}_n^{(1)}\right\} = \arg\max_{w} \left\{\sum_{k,j=1}^{n} \left| r_{k,j}^{(1)} \right|^2 + \lambda \cdot \sum_{k=1}^{n} \left| r_{k,ref}^{(1)} \right|^2\right\} \tag{2}$$

$$\text{Stage 2: for } i = 2{:}\,M \quad \left\{\boldsymbol{w}_1^{(i)}, \boldsymbol{w}_2^{(i)}, \cdots, \boldsymbol{w}_n^{(i)}\right\} = \arg\max_{w} \left\{\sum_{k,j=1}^{n} \left| r_{k,j}^{(i)} \right|^2 + \lambda \cdot \sum_{k=1}^{n} \left| r_{k,ref}^{(i)} \right|^2\right\} \tag{3}$$

$$\text{s.t. } \boldsymbol{w}_k^{(i)} \perp \left\{\boldsymbol{w}_k^{(1)}, \boldsymbol{w}_k^{(2)}, \cdots, \boldsymbol{w}_k^{(i-1)}\right\}, k = 1,2,\cdots,n$$

end

where $\boldsymbol{w}_k^{(i)} (i = 1, \dots, M)$ is the i^{th} column of the $\boldsymbol{w}$ matrices, $r_{i,j}^{(i)} = \text{corr}\left(A_k^{(i)}, A_k^{(j)}\right)$ is the correlation between the i^{th} column $\boldsymbol{A}_k$ and $\boldsymbol{A}_j$, $r_{i,ref}^{(i)}$ is the correlation between the i^{th} column of $\boldsymbol{A}_k$ and the reference signal, which has the same length of subject numbers. λ is the regularization parameter that balances the weight of $\sum_{k,j=1}^{n} \left| r_{k,j}^{(1)} \right|^2$ and $\sum_{k=1}^{n} \left| r_{k,ref}^{(1)} \right|^2$ which is usually in the range of [0.1, 1] . Particularly, MCCAR+jICA degenerates to MCCA+jICA when $\lambda = 0$. Based on the above optimization, we can obtain$\boldsymbol{A}_1, \boldsymbol{A}_2, \boldsymbol{A}_3$ simultaneously, which satisfies

$$\boldsymbol{E}\{\boldsymbol{A}_k^{\mathrm{T}} \boldsymbol{A}_k\} = \boldsymbol{I}, \boldsymbol{E}\{\boldsymbol{A}_k^{\mathrm{T}} \boldsymbol{A}_k\} \approx \text{diag}\left(r_{k,j}^{(1)}, r_{k,j}^{(2)}, \dots, r_{k,j}^{(M)}\right), k \neq j, k, j \in \{1,2,3\} \tag{4}$$

As shown in Figure1, in our case, n=3; $k \neq j; k, j = 1,2,3$, we shown an example when $M = 5$, including the source separation (Fig 1c) and inter-modality covariations (Fig 1d). In addition, one or more joint components will have significant correlations with the reference, as the 3rd component in Fig 1(c), which may be higher or equivalent in values than using MCCA only or using unimodal voxel-wise correlations (resulting in correlated ROI), as shown in Fig1(e).

B. jICA

Although MCCAR may provide a useful decomposition in many cases, the associated maps $\boldsymbol{C}_k$ may still not be unique in some cases. In order to maximize their spatial independence and ensure the available mixing references derived from MCCAR, we further apply jICA on the concatenated maps $[\boldsymbol{C}_1, \boldsymbol{C}_2, \dots, \boldsymbol{C}_n]$ to obtain the final independent sources $\boldsymbol{S}_k$, and the final mixing matrices for each modality:

$$\boldsymbol{A}_k \cdot \boldsymbol{W}^{-1}$$

$$\boldsymbol{W}[\boldsymbol{C}_1, \boldsymbol{C}_2, \cdots, \boldsymbol{C}_n] = [\boldsymbol{S}_1, \boldsymbol{S}_2, \cdots, \boldsymbol{S}_n] \tag{5}$$

$$\boldsymbol{X}_k = (\boldsymbol{A}_k \cdot \boldsymbol{W}^{-1}) \cdot \boldsymbol{S}_k \tag{6}$$

III. Simulation

We next simulated multimodal MRI data to compare the proposed method with its alternatives for its capability to extract accurate spatial maps and correspondence between multiple modalities and with the reference. 8 brain networks were simulated using the simTB [9] for fMRI and sMRI. DMRI was generated using the JHU white matter atlas in which we selected 8 typical fiber bundles, as shown in

Figure2 (A) (red boxed components are designed to correlate with reference). Loading matrices for each modality, $\boldsymbol{A}_1$, $\boldsymbol{A}_2$, $\boldsymbol{A}_3$ were constructed in size of 300×8, resulting in 300 samples with 21025, 40000 and 65536 voxels for fMRI, dMRI and sMRI feature matrices respectively by linear combination. 16 noise levels were also simulated with peak signal-to-noise ratio (PSNR) ranges from 1 dB to 34dB. Typical PSNR value for the acceptable image quality is about 30 dB; the lower the value, the more degraded the image [10]. Here, we used a real cognitive score of 300 subjects as a reference and carefully designed one component for each modality (in different order) to be significantly correlated with the reference. The accuracy used here is defined as the correlation between the true source(s)/mixing matrix and the estimated component(s)/mixing matrix.

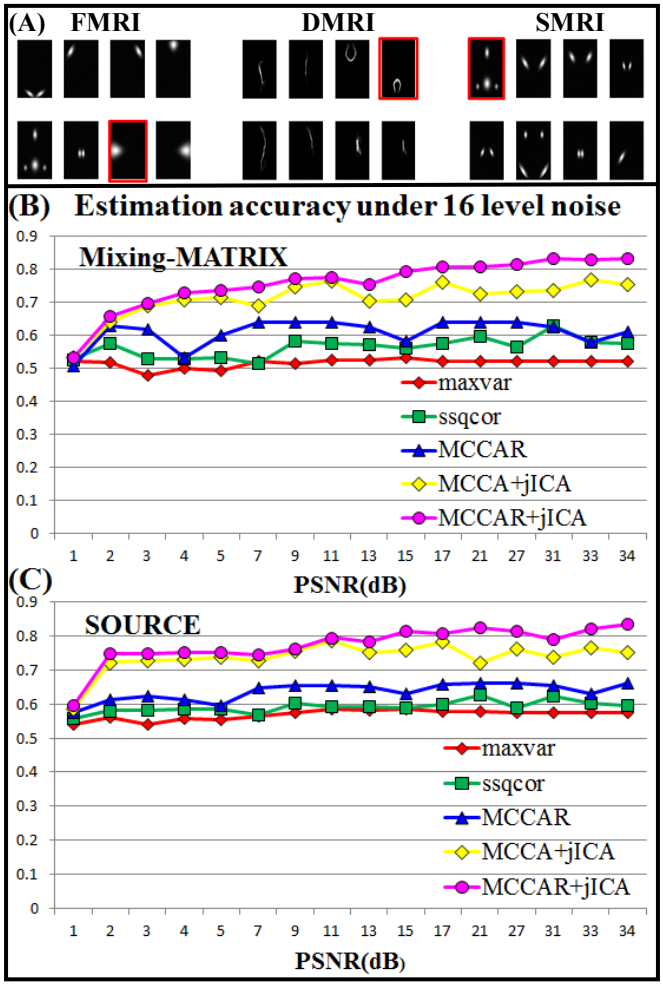

Figure 2 The simulated 8 components of 3 modalities and the comparison of estimation accuracy under 16 level noises.

We compared MCCAR+jICA with MCCA (including maxvar, ssqcor), MCCAR, MCCA+jICA and separate ICA (3ICA) on the simulated data, separately. Figure2 (B) and (C) compares the accuracy performance of sources and mixing matrix for different noise levels (averaged across 16 noise levels). It is evident that MCCAR+jICA is quite robust to noise and its source separation performance is consistently the best in all noise conditions. MCCA+jICA is the second best in source and mixing matrix estimation. Finally, the performance of MCCAR is not as good as MCCAR+jICA, which demonstrates the necessity of applying jICA.

(A) The ability of getting joint components

PSNR=7	fMRI			dMRI			sMRI		
Correlation with ref	r	p	ICth	r	p	ICth	r	p	ICth
real corr	-0.253	0.011	7	-0.263	0.008	4	-0.250	0.012	1
maxvar	-0.199	0.047	5	-0.199	0.048	2	-0.256	0.010	5
ssqcor	-0.247	0.013	7	-0.199	0.047	1	-0.250	0.012	7
MCCAR	-0.252	0.011	1	-0.281	0.005	1	-0.287	0.006	1
MCCA+jICA	0.233	0.020	4	-0.257	0.01	2	-0.249	0.013	3
				-0.221	0.027	5			
MCCAR+jICA	-0.264	0.008	1	-0.274	0.005	1	-0.265	0.008	1

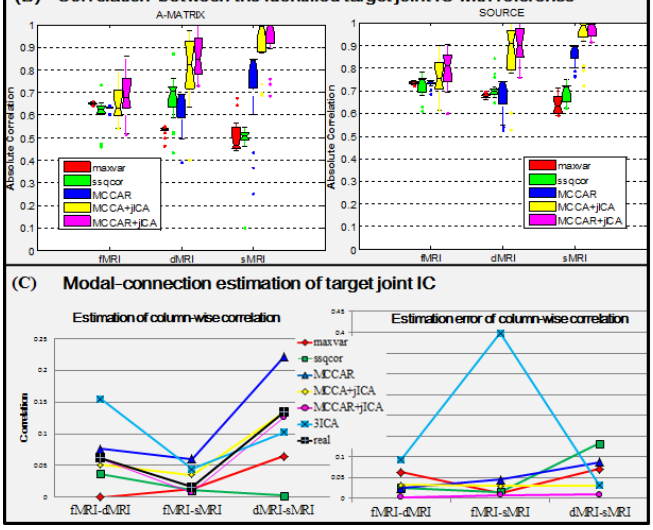

Figure 3 Comparison of different approaches in a simulated 3-way fusion.

Figure3 (A) shows the ability for different fusion methods in getting priority-set reference signals as one joint independent component (IC) under the noise condition (PSNR=7). It is clear that only supervised method MCCAR (blue) and MCCAR+jICA (pink) could obtain one joint component with right correspondence (same IC order, showing that they are all correlated with ref). But blind fusion algorithms may lose detection of the reference target as an integrative IC in noisy conditions. Figure3 (B) displays the modality-specific correlations of sources and mixing matrix between the identified targeted ICs (significantly correlated with reference) and their ground truth under 16 noise levels. It is evident that MCCAR+jICA (pink) exhibit better estimation accuracy than others on both source and mixing matrix for 3 modalities. Figure3 (C) compares the estimation of column-wise correlation and the absolute error of column-wise correlation of the identified joint component by different methods. Comparing separate ICA in each modality, MCCAR+jICA achieves best modal-connection estimation with minimum absolute error with ground truth, validating the advantages of the supervised, goal-directed multimodal fusion. In order to determine the optimal value of λ, we perform a 5-fold cross validation on 300 simulated data and found that the best λ for simulation is 0.8.

IV. HUMAN BRAIN DATA

In this study, all subjects were collected from seven sites. We recruited 147 SZs (age: 39.5 ± 11.7, gender: 35F/112M) and 147 HCs (age: 37.4 ± 11, gender: 44F/103M) who were matched for age, gender, handedness, ethnicity, and have all 3 types of MRI data. The Computerized Multiphasic Interactive Neuro-cognitive System (CMINDS, launched by the National Institute of Mental Health) scores were calculated by [11], in which the WM domain scores was used as a reference to guide the investigation of multimodal co-alterations. This WM domain score was obtained from testing Letter Number Sequencing task in the CMINDS, which is also corrected with PANSS negative score r=0.59, p=9.4×10^{-7}. Written informed consent was obtained from all study participants under protocols approved by the Institutional Review Boards at each study site.

A. Preprocessing

FMRI data were preprocessed using the MRN automated analysis pipeline, whose steps are conducted in SPM 5 as follows: Motion correction; slice timing; and normalization to MNI space, including reslicing to 3 × 3 × 3 mm voxels. We further regressed out six motion parameters, white matter, and cerebrospinal fluid in denoising. The fractional amplitude of low frequency fluctuations (fALFF) was extracted to generate a map for each subject. Data were then spatially smoothed with an 8 mm full width half max (FWHM) Gaussian filter.

DMRI data were preprocessed by FMRIB Software Library and consisted of the following steps: 1) quality check with any gradient directions with excessive motion or vibration artifacts identified and removed; 2) motion and eddy current correction; 3) correction of gradient directions for any image rotation done during the previous motion correction step; and 4) calculation of diffusion tensor and scalar measures such as fractional anisotropy (FA), which were then smoothed using 8 mm FWHM Gaussian filter.

Using the unified segmentation method in SPM, sMRI were normalized to MNI space, resliced to 3 × 3 × 3 mm, and segmented into grey matter (GM), white matter, and cerebral spinal fluid. Then, the GM images were smoothed with a FWHM of 8 mm Gaussian filter. Outliers were then visually checked, corrected, and re-segmented where possible, and removed in cases where correction was not possible.

After preprocessing, the three-dimensional brain images of each subject were reshaped into a one-dimensional vector and stacked, forming a matrix ($\boldsymbol{N}_{\text{subj}} \times \boldsymbol{N}_{\text{voxel}}$) for each of the three modalities. These three matrices were then normalized to have the same average sum of squares to ensure all modalities had the same ranges. Multivariate analysis of covariance (MANCOVA) was performed on the normalized matrix ($\boldsymbol{N}_{\text{subj}} \times \boldsymbol{N}_{\text{voxel}}$) of fALFF, FA, GM respectively. According to MANCOVA results, we then regressed out age, age by site for fALFF; site, age, gender and age by site for GM; site, age and gender for FA, respectively.

B. Joint group co-alterations related to WM

When components of the same index show group differences in more than one modality, they are called joint group-discriminative ICs. We aim to discover the joint group-discriminative ICs that also significantly correlate with CMINDS WM scores. 20 components were estimated for each feature according to an improved MDL criterion. We performed two-sample t-tests on mixing coefficients of each IC for each modality.

Among the 20 derived ICs, the 6th IC was found to be the component of interest. It is not only significantly group-discriminating (p=7.4E-06, 0.001, 7.0E-09 FDR corrected), but also correlate with WM scores (r=0.296, 0.241, 0.301) for fMRI, dMRI and sMRI, respectively. Its spatial maps were transformed into Z scores, visualized at $|\mathbf{Z}| > 2$ in Figure4 (A) and adjusted as HC > SZ for all modalities on the mean of loading parameters, as the box plot shows in Figure4 (B), so that the positive Z-values (red regions) indicate higher contribution in HC than SZ and the negative Z-values (blue regions) indicate higher contribution in SZ than HC. The identified regions in IC6 are summarized in Table 1 for fALFF and GM components as well as FA (WM tracts, from John Hopkins Atlas). Figure3 (C) indicates the positive correlation between loadings of IC6 and the WM scores in three modalities (HC: red dots, SZ: blue dots); the higher loadings correspond to better memory performance. Additionally, the identified IC6 also correlates with PANSS negative scores (r=-0.229, -0.276, -0.240) for fMRI, dMRI and sMRI, respectively. No significant correlation was found with PANSS positive scores.

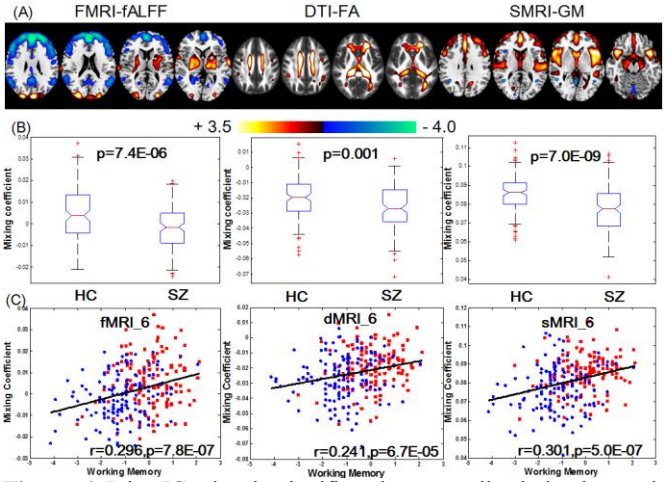

Figure 4 Joint ICs that is significantly group-discriminating and correlating with WM.

Commonly in fMRI_IC6 and sMRI_IC6, SZ showed lower values in thalamus, which is believed to be the mediator of attention under the notable contextual and leading influence of the neocortex [12] . Thalamus has dense reciprocal projections with cerebral neocortex and with limbic structures, and forms a key part of the pathway for transmission of sensory information to cortex [13]. The thalamus and the basal ganglia are key structures linked to the prefrontal cortex and are known to be involved in WM [14] and it also participate in the thalamic–cortical–striatal circuitry subserving WM [15]. An alternative account of the present findings, which emphasizes the fractional similarity network analysis results, posits the DLPFC/ACC/thalamus triad as a core deficit, with the dysfunction elsewhere in the network as a downstream functional consequence of WM disturbance [16]. The dorsolateral prefrontal cortex (DLPFC) abnormalities were both detected in fMRI_IC6 and sMRI_IC6, where patients indicated higher fALFF values but

lower GM volume. There is very consistent evidence that SZ have difficulty with processes attributed to the central executive component of WM. Two meta-analyses on WM-related brain activation in schizophrenia provide consistent evidence for altered activity in DLPFC [1, 16, 17]. Several lines of evidence suggest WM and the DLPFC component in particular, as a critical domain of dysfunction in the pathophysiology of schizophrenia. In sMRI studies, the DLPFC is a key cortical region in which gray matter is reduced in volume in schizophrenia, changes that are correlated with negative symptom severity in patients. Overall, our results suggest that higher fALFF but lower GM volume in DLPFC relates to worse cognition especially WM in schizophrenia [18].

Table 1 Anatomical Information of the Identified Joint Component in IC6

fMRI_fALFF Area	Brodmann Area	volume (cc)	random effects: Max Value Z(x, y, z)
HC>SZ			
Thalamus		0.4/0.1	2.2 (-15, -14, 3)/2.0 (12, -11, 3)
Middle Occipital Gyrus	18, 19	1.0/0.7	2.5 (-27, -87, 15)/2.3 (27, -89, 21)
SZ>HC			
Superior/Medial Frontal Gyrus	6, 8, 9, 10	19.8/19.1	3.9 (-3, 51, 28)/4.3 (3, 51, 28)
Middle Frontal Gyrus	6, 8, 9, 10, 46	13.2/12.9	3.4 (-18, 20, 57)/3.6 (27, 34, 45)
Inferior Parietal Lobule	40	1.3/0.0	2.4 (-50, -44, 44)/ NA
Inferior Frontal Gyrus	9, 45, 46	1.4/0.1	2.4 (-50, 19, 21)/2.1 (50, 24, 21)
Superior/ Middle Temporal Gyrus	22, 39	0.7/0.1	2.2 (-50, -54, 25)/2.1 (50, -57, 28)
DTI_FA WM tracts	**vol(cc)**	**Percentage**	**Zmax(R/L)**
HC>SZ			
Forceps major/minor	19.8/28.2	35%/56%	4.4(33,49,22)/3.5(32,25,22)
Inferior longitudinal fasciculus	15.9/17.5	37%/37%	2.9(10,35,6)/4.2(44,30,10)
Superior longitudinal fasciculus	21.7/26.2	23%/25%	5.4(24,33,27)/6.3(44,32,8)
sMRI_GM Area	**Brodmann Area**	**volume (cc)**	**random effects: Max Value (x, y, z)**
HC>SZ			
Superior Temporal Gyrus	13, 22, 38, 42	9.6/6.8	6.3 (-45, 11, -6)/5.1 (48, 11, -6)
Inferior Frontal Gyrus	9, 10, 13, 44, 45, 46, 47	7.1/5.8	5.8 (-42, 14, -6)/5.0 (45, 14, -6)
Insula	13, 22, 41, 47	5.3/3.3	5.7 (-45, 6, -5)/4.7 (45, 8, -5)
Medial Frontal Gyrus	6, 8, 9, 10, 11, 25, 32	4.4/4.8	3.9 (-3, 50, 9)/3.7 (3, 47, 11)
Caudate		1.0/0.9	3.4 (-6, 12, 2)/3.4 (6, 15, -1)
Parahippocampal Gyrus	28, 34, 35	0.8/0.9	2.7 (-18, -18, -14)/3.1 (15, -9, -15)
Superior /Middle Frontal Gyrus	6, 8, 9, 10,46	7.1/2.4	3.0 (-33, 48, 25)/2.6 (27, 59, 14)
Middle Temporal Gyrus	21	1.1/0.6	2.9 (-48, -35, 2)/2.4 (50, -35, -1)
Thalamus		0.0/0.4	NA/2.5 (3, -14, 6)

For fMRI only, patients indicated higher fALFF values in superior frontal gyrus (SFG), medial frontal gyrus (MFG), middle temporal gyrus (MTG), and inferior parietal lobule (IPL). Both fronto-temporal and front-parietal circuits' abnormalities were observed in fALFF. Fronto-temporal dysconnectivity has been proposed as a mechanism leading to the psychotic symptoms, especially auditory hallucinations, in schizophrenia. Disrupted fronto-parietal circuit may account for the impaired executive function and cognitive control in schizophrenia, especially the working memory deficit [19].

For GM only, patients have lower GM volume in insular, caudate, amygdala, hippocampus, and superior temporal gyrus (STG). Insular is a cortical structure with extensive connections to many areas of the cortex and limbic system. It integrates external sensory input with the limbic system and is integral to the awareness of the body's state (interoception) [20]. Many deficits observed in schizophrenia involve these functions and may relate to insula pathology. We successfully replicated the previous studies that a relatively greater degree of reduction in frontal and temporal cortical volumes in schizophrenia has been extracted.

For dMRI, the co-occurring FA values in superior longitudinal fasciculus (SLF), inferior longitudinal fasciculus (ILF), forceps minor (FMIN) and forceps major (FMAJ) were lower in SZ. The FMAJ linking DLPFC region is traversed by tracts interconnecting the frontal lobe, providing evidence for disrupted anatomical connections in the fronto-limbic circuitry, even at the early stages of schizophrenia [21]. FA changes in the SLF, the major white matter connection between prefrontal and parietal cortices, relate to verbal WM performance [22]. The integrity of this physiological connection predicted performance on a verbal WM task, indicating that this structural change may have important functional implications. It is also worth noting that the SLF is a late-maturating tract [21]. According to the macrocircuit theory, specific white matter tracts are disrupted either as a cause or a consequence of a disorder in the gray matter regions they connect. Consistent with previous reports, the current study also found moderate correlations between the severity of negative symptom and diffusion measurements of certain tracts, including FMAJ, FMIN, SLF, and ILF [21].

C. *Future directions*

Overall, our studies offer a new strategy to link cognition and multimodal neuroimaging data. Other cognitive domains beyond WM could also be studied using our method, *e.g.* attention [23]. In addition, the choice of cognitive measure is flexible. In addition to the CMINDS cognitive assessment, there are other assessment tools that we can use to provide prior guidance for fusion, for instance, the Cambridge Neuropsychological Test Automated Battery (CANTAB) [24] used in Parkinson's Disease; MCCB [25]; and symptom severity scores to search for a relationship between neuroimaging and symptomatology. Furthermore, MCCAR+jICA can be applied to study other brain diseases (such as psychotic major depression disorder (MDD), or non-psychotic bipolar disorder (BP)). Finally, apart from the above mentioned cognitive measures, genetic data could also be used as reference, *e.g.* a single gene locus, or a micro RNA, to explore genetic variants associated with brain structure and function, presenting a new means of mapping genetic influences on mental disorders. We plan to pursue this possibility in our future work.

D. *Conclusion*

In summary, we proposed a novel supervised multivariate data-driven approach, MCCAR+jICA, which is designed to extract interested components correlating with a specific prior reference. This study also provides proof-of-concept for the application of the proposed method in brain imaging data. Simulations indicate that MCCAR+jICA is proved to be able to extract the targeted components with improved accuracy. In a real-world fusion application, we successfully identified a joint group-discriminating component that is also correlated with CMINDS WM scores. Furthermore, the identified spatial maps replicated previous findings on the abnormal brain regions related to WM dysfunction in schizophrenia. This means in real human brain imaging applications, we could

simultaneously exploring goal-directed multimodal co-alterations and associations with specific clinical measures, which promise a widely use in the future neuroimaging community.

V. ACKNOWLEDGMENT

This work was supported by the National High-Tech Development Plan of China (863) (No. 2015AA020513), the Strategic Priority Research Program of the Chinese Academy of Sciences (Grant No. XDB02060005), "100 Talents Plan" of Chinese Academy of Sciences, and China National Science Foundation Number 81471367; and NIH grants P20GM103472, R01EB006841 and R01EB005846.

VI. REFERENCES

[1] J. L. a. S. Park, "Working memory impairments in schizophrenia A meta-analysis," *J Abnorm Psychol,* vol. 114, no. 4, pp. 599-611, 2005.

[2] J. Sui, H. He, G. D. Pearlson, T. Adali, K. A. Kiehl, Q. Yu, V. P. Clark, E. Castro, T. White, B. A. Mueller, B. C. Ho, N. C. Andreasen, and V. D. Calhoun, "Three-way (N-way) fusion of brain imaging data based on mCCA+jICA and its application to discriminating schizophrenia," *Neuroimage,* vol. 66, pp. 119-32, Feb 1, 2013.

[3] J. Sui, G. Pearlson, A. Caprihan, T. Adali, K. A. Kiehl, J. Liu, J. Yamamoto, and V. D. Calhoun, "Discriminating schizophrenia and bipolar disorder by fusing fMRI and DTI in a multimodal CCA+ joint ICA model," *Neuroimage,* vol. 57, no. 3, pp. 839-55, Aug 1, 2011.

[4] Y. L.-S. Tulay Adali, and Vince D. Calhoun, "Multimodal Data Fusion Using Source Separation: Two Effective Models Based on ICA and IVA and Their Properties," *Proc IEEE Inst Electr Electron Eng* vol. 103, pp. 1478-1493, 2015.

[5] J. Liu, G. Pearlson, A. Windemuth, G. Ruano, N. I. Perrone-Bizzozero, and V. Calhoun, "Combining fMRI and SNP data to investigate connections between brain function and genetics using parallel ICA," *Hum Brain Mapp,* vol. 30, no. 1, pp. 241-55, Jan, 2009.

[6] V. M. Vergara, A. Ulloa, V. D. Calhoun, D. Boutte, J. Chen, and J. Liu, "A three-way parallel ICA approach to analyze links among genetics, brain structure and brain function," *Neuroimage,* vol. 98, pp. 386-94, Sep, 2014.

[7] V. D. Calhoun, and J. Sui, "Multimodal fusion of brain imaging data: A key to finding the missing link(s) in complex mental illness," *Biological Psychiatry: Cognitive Neuroscience and Neuroimaging,* vol. In press, 2016.

[8] J. Sui, T. Adali, Q. Yu, J. Chen, and V. D. Calhoun, "A review of multivariate methods for multimodal fusion of brain imaging data," *J Neurosci Methods,* vol. 204, no. 1, pp. 68-81, Feb 15, 2012.

[9] E. B. Erhardt, E. A. Allen, Y. Wei, T. Eichele, and V. D. Calhoun, "SimTB, a simulation toolbox for fMRI data under a model of spatiotemporal separability," *Neuroimage,* vol. 59, no. 4, pp. 4160-7, Feb 15, 2012.

[10] N. Thomos, Boulgouris, N.V., Strintzis, M.G., "Optimized transmission of JPEG2000 streams over wireless channels," *IEEE Trans. Image Process,* vol. 15, 2006.

[11] T. G. Van Erp, A. Preda, J. A. Turner, S. Callahan, V. D. Calhoun, J. R. Bustillo, K. O. Lim, B. Mueller, G. G. Brown, J. G. Vaidya, S. McEwen, A. Belger, J. Voyvodic, D. H. Mathalon, D. Nguyen, J. M. Ford, S. G. Potkin, and Fbirn, "Neuropsychological profile in adult schizophrenia measured with the CMINDS," *Psychiatry Res,* vol. 230, no. 3, pp. 826-34, Dec 30, 2015.

[12] D. Pinault, "Dysfunctional thalamus-related networks in schizophrenia," *Schizophr Bull,* vol. 37, no. 2, pp. 238-43, Mar, 2011.

[13] C. G. W. Robert W. McCarley, Melissa Frumin, Yoshio Hirayasu, James J. Levitt, Iris A. Fischer, and Martha E. Shenton, "MRI Anatomy of Schizophrenia," *Biological Psychiatry,* vol. 45, pp. 1099-1119, 1999.

[14] J. Bor, J. Brunelin, D. Sappey-Marinier, D. Ibarrola, T. d'Amato, M. F. Suaud-Chagny, and M. Saoud, "Thalamus abnormalities during working memory in schizophrenia. An fMRI study," *Schizophr Res,* vol. 125, no. 1, pp. 49-53, Jan, 2011.

[15] D. N. B. Stan B. Floresco, and Anthony G. Phillips, "Thalamic–Cortical–Striatal Circuitry Subserves Working Memory," *The Journal of Neuroscience,* vol. 19, pp. 11061–11071, 1999.

[16] A. R. L. Michael J. Minzenberg, Sarah Thelen, Cameron S. Carter, David C. Glahn, "Meta-analysis of 41 Functional Neuroimaging Studies of Executive Function in Schizophrenia," *Arch Gen Psychiatry,* vol. 66, no. 8, pp. 811-822, 2009.

[17] D. C. Glahn, J. D. Ragland, A. Abramoff, J. Barrett, A. R. Laird, C. E. Bearden, and D. I. Velligan, "Beyond hypofrontality: a quantitative meta-analysis of functional neuroimaging studies of working memory in schizophrenia," *Hum Brain Mapp,* vol. 25, no. 1, pp. 60-9, May, 2005.

[18] J. Sui, G. D. Pearlson, Y. Du, Q. Yu, T. R. Jones, J. Chen, T. Jiang, J. Bustillo, and V. D. Calhoun, "In Search of Multimodal Neuroimaging Biomarkers of Cognitive Deficits in Schizophrenia," *Biol Psychiatry,* vol. 78, no. 11, pp. 794-804, Dec 1, 2015.

[19] Y. Zhou, L. Fan, C. Qiu, and T. Jiang, "Prefrontal cortex and the dysconnectivity hypothesis of schizophrenia," *Neurosci Bull,* vol. 31, no. 2, pp. 207-19, Apr, 2015.

[20] K. P. Wylie, and J. R. Tregellas, "The role of the insula in schizophrenia," *Schizophr Res,* vol. 123, no. 2-3, pp. 93-104, Nov, 2010.

[21] H. Sun, S. Lui, L. Yao, W. Deng, Y. Xiao, W. Zhang, X. Huang, J. Hu, F. Bi, T. Li, J. A. Sweeney, and Q. Gong, "Two Patterns of White Matter Abnormalities in Medication-Naive Patients With First-Episode Schizophrenia Revealed by Diffusion Tensor Imaging and Cluster Analysis," *JAMA Psychiatry,* vol. 72, no. 7, pp. 678-86, Jul, 2015.

[22] K. H. Karlsgodt, T. G. van Erp, R. A. Poldrack, C. E. Bearden, K. H. Nuechterlein, and T. D. Cannon, "Diffusion tensor imaging of the superior longitudinal fasciculus and working memory in recent-onset schizophrenia," *Biol Psychiatry,* vol. 63, no. 5, pp. 512-8, Mar 1, 2008.

[23] M. D. Rosenberg, E. S. Finn, D. Scheinost, X. Papademetris, X. Shen, R. T. Constable, and M. M. Chun, "A neuromarker of sustained attention from whole-brain functional connectivity," *Nat Neurosci,* vol. 19, no. 1, pp. 165-71, Jan, 2016.

[24] M. N. Levaux, S. Potvin, A. A. Sepehry, J. Sablier, A. Mendrek, and E. Stip, "Computerized assessment of cognition in schizophrenia: promises and pitfalls of CANTAB," *Eur Psychiatry,* vol. 22, no. 2, pp. 104-15, Mar, 2007.

[25] B. Kirkpatrick, W. S. Fenton, W. T. Carpenter, Jr., and S. R. Marder, "The NIMH-MATRICS consensus statement on negative symptoms," *Schizophr Bull,* vol. 32, no. 2, pp. 214-9, Apr, 2006.